Preprints of the 21st IFAC World Congress (Virtual)
Berlin, Germany, July 12-17, 2020

Adaptive RBF Neural Network Control Method for Pneumatic Position Servo System ⋆

Hai-Peng Ren * **Shan-Shan Jiao** * **Xuan Wang** * **Jie Li** **

* *Shaanxi Key Laboratory Complex System Control and Intelligent Information Processing, Xi'an University of Technology, Xi'an, China (e-mail: renhaipeng@xaut.edu.cn).*
** *School of Electrical Engineering, Xi'an University of Technology, Xi'an, China (e-mail: lijie@xaut.edu.cn).*

Abstract: With the development of control theory and the pneumatic element, the application of pneumatic systems has attracted more attention because of the performance to price ratio improvement. Despite of these, there are still challenge to deal with the nonlinearity of the system, the uncertainty of the parameters, the input saturation and the unknown control direction in the tracking control of pneumatic system. In this paper, the nonlinearity and model uncertainty are treated with adaptive radial basis function neural network (RBFNN), meanwhile, the unknown control direction and input saturation are dealt with the Nussbaum function and Gauss error function, respectively. The stability of the designed controller is proved by Lyapunov theory. Finally, the experimental and comparison results show the effectiveness and superiority of the proposed method.

Keywords: Pneumatic system, RBFNN, unknown model parameters, unknown control direction, input saturation.

1. INTRODUCTION

Pneumatic systems are widely used in industrial automation in the world due to their cleanness, simple structure and anti-electromagnetic interference [Yong and Wang (2009)]. However, due to the compressibility of air, the low natural frequency of pneumatic systems, the complex flow through the valve port. It is very difficult to improve positioning and tracking accuracy [Bai (2014)]. Therefore, it is necessary to develop appropriate control methods to improve the efficiency of pneumatic systems.

In recent years, many scholars have applied nonlinear system control methods and intelligent control methods to pneumatic systems [Yamamoto and Araki (1999)]. Among them, adaptive control achieved a good control performance when parameters can not be exactly determined [**?**]. [Li et al. (1998)] used single neuron adaptive PID control, and achieved high positioning accuracy; [Yamamoto and Araki (1999)] used a model reference adaptive control method to control the pneumatic servo system. At the same time, adaptive control and backstepping design are often combined to eliminate the influence of system parameter time-varying and various disturbances. [Ren and Huang (2013a), Ren and Huang (2013b)] proposed two adaptive backstepping controllers. The design of the controller adopted the backstepping method, by constructing the Lyapunov function to design the virtual control, and to prove the stability of the system. [Ren and Fan (2016)] designed an adaptive backstepping controller by combining Nussbaum function gain with adaptive backstepping design method for pneumatic systems with unknown model parameters and control gain symbols. Neural network control mainly uses the function approximation function of neural network to achieve effective control of nonlinear objects. [Choi et al. (1998)]used neural networks to deal with the nonlinear relationship between velocity and acceleration during penumatic system motion; [Dehghan and Surgenor (2013)] designed the neural network PID control and achieved good control performance. Furthermore, the combination of neural network control and adaptive control can overcome the influence of the nonlinearity of pneumatic systems. [Sakamoto et al. (2002)] pointed out that, due to the compressibility of air and the nonlinearity caused by cylinder friction, the model reference adaptive control algorithm combined with neural network improved the system performance; Based on the traditional I-PD control algorithm, [Fujiwara et al. (1995)] used the neural network to learn the automatic adjustment of I-PD gain, and proposed a self-correcting I-PD controller, this method was applied in the position control of the cylinder and achieved good tracking performance; [Li and Tanaka (2003)] proposed an adaptive pole placement control based on neural network, so that the nonlinear system linearization can be realized. These studies contribute the application of the pneumatic system. At present, the performance of the tracking control of pneumatic systems

⋆ This work was supported in part by the Shaanxi Provincial Special Support Program for Science and Technology Innovation Leader, in part by the Shaanxi Industrial Key Project (2018GY-165), and in part by Key Lab Research Program from Department of Education of Shaanxi Provincial Government (18JS081).

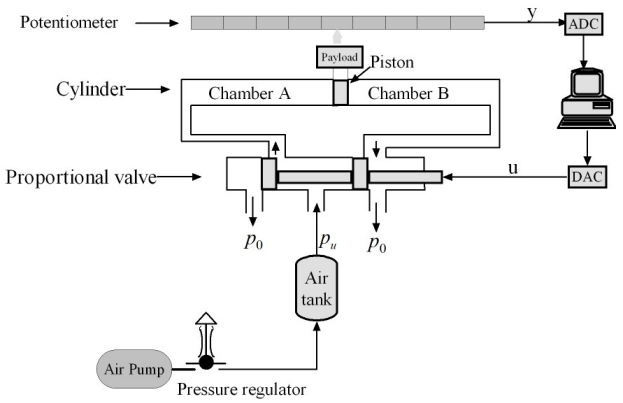

Fig. 1. Pneumatic servo control experiment system

needs to be further improved using the high performance control method.

In this paper, an adaptive neural network [Zhai et al. (2008)] based control method is proposed for pneumatic servo systems with input saturation and unknown direction control. In this method, the neural network and adaptive backstepping method are combined with Nussbaum function and Gauss error function for tracking control of the pneumatic tracking control system. The RBFNN is used to approximate the unknown nonlinear function. Finally, the Lyapunov function is utilized to prove the stability of the system, at the same time, the controller and parameter adaptive law are designed. The experimental results show that, when the control direction of the system changes, the designed adaptive RBFNN controller can track three kinds of reference signals very well. Compared with some existing methods, this method obtains better control performance.

2. THE MODEL OF PNEUMATIC SYSTEM AND RBFNN

2.1 Pneumatic System Configure and Its Model

The principle of the pneumatic position servo system is shown in Fig. 1. The compressed air is supplied by the air compression pump, the flow of the compressed air into chamber is controlled by the proportional valve, a pressure difference created by the chamber causes the movement of the payload. The displacement signal is sent to the computer and the control signal is fed into the proportional valve through the A/D and D/A converter of the data acquisition card, respectively. Finally, the closed-loop control is realized.

The dynamic equation of the pneumatic position servo system is:

$$p_a A_a - p_b A_b - F_f = M\ddot{y}, \tag{1}$$

where $\ddot{y}$ is the piston motion acceleration. F_f is the sum of static friction, Coulomb friction, and viscous friction. M is the total mass of the piston and payload. p_a and p_b are pressures in Chambers A and B, respectively.

The model of system is given by [Ren and Fan (2016), Choi et al. (1998), Bone and Ning (2007)].

$$\begin{cases} \dot{m}_a = q_{ma} \\ \dot{m}_b = q_{mb} \\ KRT\dot{m}_a = Kp_a A_a \dot{y} + A_a(y_0 + y)\dot{p}_a \\ KRT\dot{m}_b = -Kp_b A_b \dot{y} + A_b(y_0 - y)\dot{p}_b \\ M\ddot{y} = p_a A_a - p_b A_b - F_f \end{cases}, \tag{2}$$

where $\dot{m}_a$ and $\dot{m}_b$ are the gas mass flow rates into Chambers A and B. A_a and A_b are the effective cross section in the chamber A and B, respectively. y_0 is the initial position of the payload. $\dot{y}$ is the velocity of the payload. K is the specific heat ratio. T is the air temperature. R is the ideal gas constant. q_{ma} and q_{mb} are the mass flow rates of gas flowing into the cylinder chamber A and chamber B, respectively, which are given as:

$$\begin{cases} q_{ma} = \sqrt{p_u - p_a}(c_{a1}u + c_{a2}u^2) \\ q_{mb} = \sqrt{p_b - p_0}(c_{b1}u + c_{b2}u^2) \end{cases}, \tag{3}$$

where p_0 is the atmospheric pressure, p_u is the upstream pressure, $c_{a1}, c_{a2}, c_{b1}, c_{b2}$ are constants related to the air property, u is the input voltage of the proportional valve.

Define the displacement of the payload as $x_1 = y$, the velocity of the payload as $x_2 = \dot{y}$ and the acceleration of the payload as $x_3 = \ddot{y}$. Linearize of q_{ma} and q_{mb} and treat the friction F_f and other unmodeled factors as disturbance, the third-order linear model of the pneumatic position servo system can be obtained as follows [Ren and Huang (2013a), Ren and Huang (2013b)]:

$$\begin{cases} \dot{x}_1 = x_2 \\ \dot{x}_2 = x_3 \\ \dot{x}_3 = a_1 x_1 + a_2 x_2 + a_3 x_3 + bu + d \\ y = x_1 \end{cases}, \tag{4}$$

where a_1, a_2, a_3 and b are the model parameters, d is the disturbance.

2.2 RBFNN

RBFNNs are usually used to approximate the unknown nonlinear and continuous functions due to their approximation capabilities. They can approximate functions with the above characteristics over a specified compact set to any arbitrary accuracy. The RBFNN is a three-layer forward neural network [Chen et al. (2015)]. Its specific structure is shown in the Fig. 2.

Input layer: As a function of the input signal $G = [g_1, g_2, ..., g_q]^T \in R^q, l = 1, 2, ..., q$ to the hidden layer, the input layer is directly fed into the hidden layer with weight being 1.

Hidden layer: Each hidden layer node contains a center vector cc, the Euclidean distance between g_l and cc_j is defined as $\|g_l - cc_j\|$. The output of the hidden layer is given as:

$$S_j(G) = e^{-\frac{\|G - cc_j\|}{\sigma_j^2}}, \tag{5}$$

where σ_j is the width of the Gauss function, $j = 1, 2, ..., m$ is the number of nodes in the hidden layer, $S(G) = [S_1(G), S_2(G), ..., S_m(G)]^T \in R^m$.

Output layer: The output of the network is shown by the following linear weighting function:

$$Y(G) = W^T S(G), \tag{6}$$

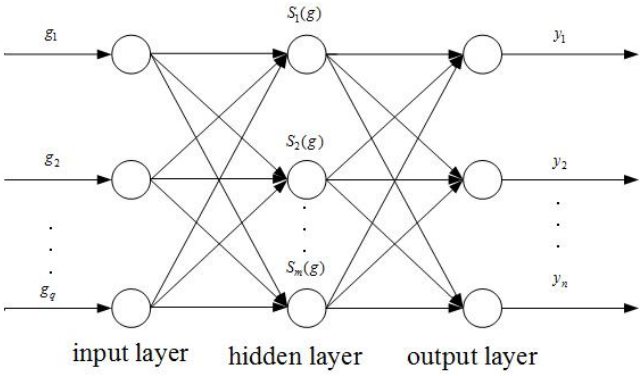

Fig. 2. RBFNN structure

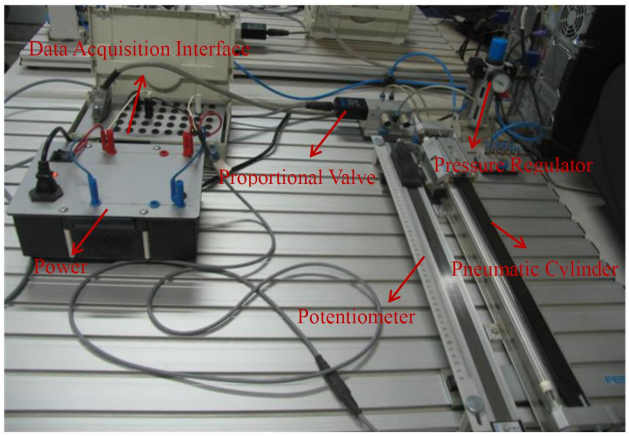

Fig. 3. Experiment equipments

where $W \in R^m$ is the weight vector of output layer, $Y(G) = [y_1, y_2, ..., y_n]^T$, y_i is the neural network output, $i = 1, 2, ..., n$ is the number of output nodes.

3. ADAPTIVE RBFNN CONTROLLER DESIGN BASED ON BACKSTEPPING METHOD

3.1 Saturated Pneumatic System Model

In this paper, Gauss error function $erf(x)$ is used to describe a class of saturation nonlinearity, which is defined as[Ma et al. (2015)]

$$erf(x) = \frac{2}{\sqrt{\pi}} \int_0^x e^{-t^2} dt, \tag{7}$$

$erf(\cdot)$ is a real-valued and continuous differentiable function.

According equation (7), the model to represent the saturation nonlinearity with smooth form can be obtained as

$$u' = u_M \times erf(au), \tag{8}$$

where u_M is a known bound of u, $a = \sqrt{\pi}/(2u_M)$, it can be easily adjusted to different lower and upper bounds by alternating the valve u_M in equation (8).

Substituting equation (8) into equation (4), we have:

$$\begin{cases} \dot{x}_1 = x_2 \\ \dot{x}_2 = x_3 \\ \dot{x}_3 = a_1 x_1 + a_2 x_2 + a_3 x_3 + bu' + d \\ y = x_1 \end{cases}. \tag{9}$$

3.2 Adaptive RBFNN Control Design

$N(\zeta)$ is an Nussbaum type function that satisfies [Li et al. (2010)]

$$\begin{matrix} \lim\limits_{s\to\infty} \sup \frac{1}{s} \int\limits_0^s N(\zeta) d\zeta = +\infty \\ \lim\limits_{s\to\infty} \inf \frac{1}{s} \int\limits_0^s N(\zeta) d\zeta = -\infty \end{matrix}. \tag{10}$$

Lemma 1 [Ma et al. (2015)] Let $V(t)$, $\zeta(t)$ be smooth functions defined on $[0, t_f]$, **if the following inequality holds:**

$$V(t) \le c_0 + \int_0^t (bN(\zeta) + 1)\dot{\zeta} d\tau, \forall t \in [0, t_f), \tag{11}$$

where c_0 is a constant, then $\int_0^t (bN(\zeta) + 1)\dot{\zeta} d\tau$, $V(t)$ and $\zeta(t)$ must be bounded on $[0, t_f]$.

Assumption The desired trajectory y_m is continuous and its upto the nth order derivatives are known and bounded.

As we all known, the control objective is to design an adaptive RBFNN controller for pneumatic system and let the output y following a desired trajectory y_m [Meng et al. (2013), Peng et al. (2006)].

Define the tracking error as [Ren et al. (2019b), Rubio et al. (2011)]:

$$\begin{cases} z_1 = x_1 - y_m \\ z_2 = x_2 - \alpha_1 \\ z_3 = x_3 - \alpha_2 \end{cases}, \tag{12}$$

where α_1, α_2 are virtual control variables. We design an adaptive RBFNN cntroller as follows:

Step 1: Select the first Lyapunov function candidate as

$$V_1 = \frac{1}{2} z_1^2. \tag{13}$$

The derivative of equation (13) is

$$\dot{V}_1 = z_1 \dot{z}_1 = z_1 (x_2 - \dot{y}_m) = z_1 (z_2 + \alpha_1 - \dot{y}_m). \tag{14}$$

Choose the first virtual control as

$$\alpha_1 = \dot{y}_m - c_1 z_1, \tag{15}$$

where c_1 is a positive constant. if $z_2 = 0$, then $\dot{V}_1 = -c_1 z_1^2 \le 0$, as a result, the first subsystem is stable.

Step 2: Select the second Lyapunov function candidate as

$$V_2 = V_1 + \frac{1}{2} z_2^2. \tag{16}$$

The derivative of equation (16) is

$$\dot{V}_2 = \dot{V}_1 + z_2 \dot{z}_2 = z_1 z_2 - c_1 z_1^2 + z_2 (z_3 + \alpha_2 - \dot{\alpha}_1). \tag{17}$$

Choose the second virtual control as

$$\alpha_2 = \dot{\alpha}_1 - c_2 z_2 - z_1, \tag{18}$$

where c_2 is a positive constant. if $z_3 = 0$, we have $\dot{V}_2 = -c_1 z_1^2 - c_2 z_2^2 \leq 0$, then the second subsystem is stable.

Step 3: From equation (9) and equation (12), we can obtain

$$\begin{aligned} \dot{z}_3 = \dot{x}_3 - \dot{\alpha}_2 = a_1 x_1 + a_2 x_2 + a_3 x_3 + \\ bu' + d - \dot{\alpha}_2 \end{aligned} . \tag{19}$$

RBFNN is used to approximate the unknown function $f(G) = a_1 x_1 + a_2 x_2 + a_3 x_3 - \dot{\alpha}_2$, RBFNN input vector $G = [x_1, x_2, x_3, \dot{\alpha}_2]$, then

$$f(G) = \hat{W}^T S(G) - \tilde{W}^T S(G) + \varepsilon(G), \tag{20}$$

where $\varepsilon(G)$ is approximation error, $S(G)$ is a function of the input vector G, W is unknown weight, define an estimation of $\hat{W}$ as W, we can obtain estimation error $\tilde{W} = \hat{W} - W$.

Select the third Lyapunov function candidate as

$$V_3 = V_2 + \frac{1}{2} z_3^2 + \frac{1}{2} \tilde{W}^T \Gamma^{-1} \tilde{W} + \frac{1}{2o} \tilde{d}^2, \tag{21}$$

where Γ is a positive defined matrix. Define an estimation of d as $\hat{d}$, we can obtain estimation error $\tilde{d} = \hat{d} - d$.

The derivative of equation (21) is

$$\dot{V}_3 = \dot{V}_2 + z_3 \dot{z}_3 + \tilde{W}^T \Gamma^{-1} \dot{\tilde{W}} + \tfrac{1}{o} \tilde{d} \dot{\hat{d}} . \tag{22}$$

The adaptive RBFNN controller and adaptive law as follows:

$$\begin{cases} u = N(\zeta) \left[c_3 z_3 + \hat{W}^T S(G) \right] - \left(z_2 + \hat{d} \right) \Big/ b \\ N(\zeta) = \zeta^2 \cos(\zeta) \\ \dot{\zeta} = c_3 z_3^2 + z_3 \hat{W}^T S(G) \\ \dot{\hat{W}} = \Gamma \left[z_3 S(G) - \sigma \hat{W} \right] \\ \dot{\hat{d}} = o z_3 \end{cases} , \tag{23}$$

where c_3, σ and b are constants. Substituting equation (8) and equation (23) into equation (22), we obtain

$$\begin{aligned} \dot{V}_3 &= -c_2 {z_2}^2 - c_1 {z_1}^2 + z_3 (\hat{W}^T S(G) - \tilde{W}^T S(G) + \varepsilon(G)) \\ &\quad + z_2 z_3 + b z_3 u_M erf(au) + z_3 \hat{d} + \tilde{W}^T \Gamma^{-1} \dot{\tilde{W}} + \tfrac{1}{o} \tilde{d} \dot{\hat{d}} \\ &= -c_2 {z_2}^2 + z_3 (\hat{W}^T S(G) - \tilde{W}^T S(G) + \varepsilon(G)) + b N(\zeta) \dot{\zeta} \\ &\quad - c_1 {z_1}^2 + \tilde{W}^T z_3 S(G) - \sigma \tilde{W}^T \hat{W} + \dot{\zeta} - c_3 z_3^2 - z_3 \hat{W}^T S(G) \\ &= -c_2 {z_2}^2 - c_1 {z_1}^2 - c_3 z_3^2 + \dot{\zeta} (b N(\zeta) + 1) \\ &= -\sum_{i=1}^{3} c_i z_i^2 + \dot{\zeta} (b N(\zeta) + 1) \end{aligned} . \tag{24}$$

Integrate equation (24) over $[0, t]$, we obtain

$$\begin{cases} V_3(t) = V_3(0) - \sum_{i=1}^{3} c_i \int_0^t {z_i}^2 d\tau + \int_0^t (bN(\zeta) + 1) \dot{\zeta} d\tau \\ \quad \leq V_3(0) + \int_0^t (bN(\zeta) + 1) \dot{\zeta} d\tau \end{cases} . \tag{25}$$

According to *Lemma 1*, we obtain $\int_0^t (bN(\zeta) + 1) \dot{\zeta} d\tau$ and $V_3(t)$ are bounded on $[0, t_f]$. As a result, the system is stable.

4. EXPERIMENTAL RESULTS

4.1 Experimental setup

The hardware platform is shown in Fig .3. Its components include: power supply, a five-way proportional valve, a potentiometer, a double-acting rodless cylinder with a 25mm diameter bore and a 450mm stroke. The compressed air is used as the energy source. The data acquisition card

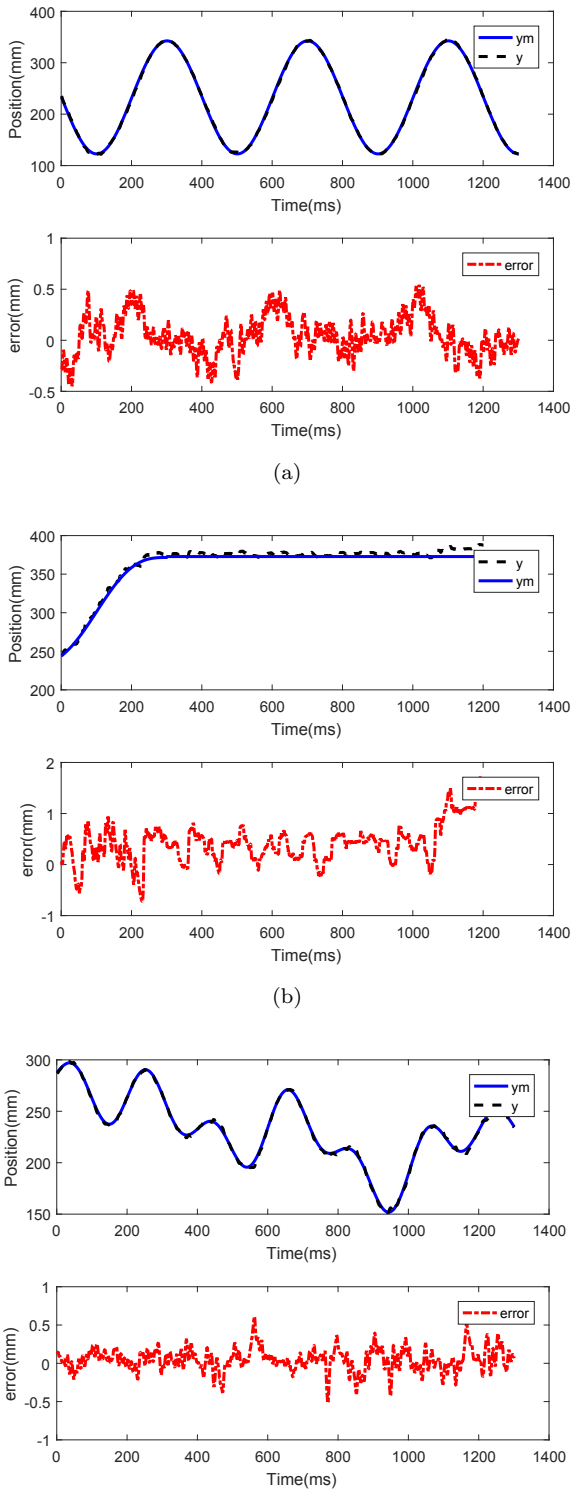

Fig. 4. Experimental results of reference signals by using the proposed method for positive control direction. In each subplot, the upper panel is the reference and output, and the lower panel is the corresponding tracking error.

PCI2306 is used for position information acquisition and proportional valve control output.

4.2 Experimental and comparison results

The analog signal output range of the D/A converter is selected from 0-10v, and its corresponding digital signal is between 0-4095. In order to decrease the energy consumption, the controller output of all methods is limited to $[-U_{\max}, U_{\max}]$. Reference signals for tracking control are the same as in[Ren et al. (2019a), Ren et al. (2019b)].

The adaptive RBFNN controller combined with Nussbaum function to solve the problem of unknown control direction. The parameters of the controller are set as $c_1 = 50, c_2 = 10, c_3 = 10, b = 0.5, o = 1000$. When the control direction is positive, the tracking results are shown as Fig. 4(a), Fig. 4(b), Fig. 4(c). The experimental results of the proposed adaptive RBFNN controller for negative direction and the comparison of the proposed method with some existing methods are given quantitively in Tables 1 to 3.

To quantitatively analyze the tracking error of these methods in steady state, we define two indices: one is the root mean square error(RMSE) of the tracking performance, another is the energy consumption (Q) during the steady state, both are the same as in [Ren and Fan (2016)]. Every experiment is done at least 30 times to avoid the influence of random factors, then the maximum value and average value of $RMSE$ and Q are obtained. From the comparison results in Table 1 to 3, we know that the proposed method achieves the superior performance as compared to some existing methods.

5. CONCLUSION

In this paper, an RBFNN controller for position tracking control of pneumatic servo system is proposed. The controller combines RBFNN with the backstepping designing, Gauss error function and Nussbaum function to solve the problems that the unknown model, unknown control direction and input saturation. This paper mainly does the following work: First, the controller proposed in this paper uses RBFNN to approximate unknown model of the pneumatic system, and the stability of the controller is proved; Second, the controller uses the Nussbaum function solves the unknown control direction of the pneumatic system; and then, the controller is combined with the Guass error function to deal with the input saturation nonlinearity problem; Finally, the controller is designed without the need for expensive pressure sensors, thereby significantly reducing costs. According to the experimental results, the proposed method is effective whether the control direction is positive or negative. Compared with some existing methods, the method decreases energy consumption and has better tracking performance.

REFERENCES

Bai, Y.H. (2014). *Pneumatic Servo System Analysis and Control*. Beijing: Metallurgical Industry Press.

Bone, G.M. and Ning, S. (2007). Experimental comparison of position tracking control algorithms for pneumatic cylinder actuators. *IEEE/ASME Transactions on Mechatronics*, 12(5), 557–561.

Bouri, M. and Thomasset, D. (2001). Sliding control of an electropneumatic actuator using an integral switching surface. *IEEE Transactions on Control Systems Technology*, 9(2), 368–375.

Chen, M., Gao, T., and Jiang, B. (2015). Dynamic surface control using neural networks for a class of uncertain nonlinear systems with input saturation. *IEEE Transactions on Neural networks and learning systems*, 26(9), 2086–2097.

Chiu, C.S. (2012). Derivative and integral terminal sliding mode control for a class of mimo nonlinear systems. *Automatica*, 48(2), 316–326.

Choi, G.S., Han, K.L., and Choi, G.H. (1998). A study on tracking position control of pneumatic actuators using neural network. In *Industrial Electronics Society, the 24th Annual Conference of the IEEE*, 1749–1753. IEEE.

Dehghan, B. and Surgenor, B.W. (2013). Comparison of fuzzy and neural network adaptive methods for the position control of a pneumatic system. In *26th IEEE Canadian Conference on Electrical and Computer Engineering (CCECE)*, May5–8, 1–4. IEEE.

Fujiwara, A., Katsumata, K., and Ishida, Y. (1995). Neural network based adaptive i-pd controller for pneumatic cylinder. In *Proceedings of the 34th SICE Annual Conference*, 1281–1284.

Li, B.R., Zhu, Y.Q., and Xu, Y.M. (1998). Adaptive control system for pneumatic position servo system. *China Mechanical Engineering*, 9(3), 4–8.

Li, J.H. and Tanaka, K.Y. (2003). Intelligent control for pneumatic servo system. *Jsme International Journal*, 46(2), 699–704.

Li, X.Q., Wang, D., Yao, Y.B., Lan, W.Y., Peng, Z.H., and Sun, G. (2010). Adaptive fuzzy control for a class of nonlinear time-delay systems with unknown control direction. In *Proceedings of the 29th Chinese Control Conference*, Beijing, China, Jul29–31, 2593–2597.

Ma, J., Zheng, Z., and Li, P. (2015). Adaptive dynamic surface control of a class of nonlinear systems with unknown direction control gains and input saturation. *IEEE Transactions on Cybernetics*, 45(4), 728–741.

Meng, D.Y., Tao, G.L., and Qian, P.F. (2013). Adaptive robust control of aerodynamic servo system. *Journal of Zhejiang University (Engineering Edition)*, 47(9), 1611–1619.

Nguyen, T., Leavitt, J., Jabbari, F., and Bobrow, J.E. (2007). Accurate slide-mode control of pneumatic systems using low-cost solenoid valves. *IEEE/ASME Transactions on Mechatronics*, 12(2), 216–219.

Peng, J.S., Wang, Q., Liu, D.L., and Song, S.L. (2006). Speed adaptive backstepping control of permanent magnet synchronous motor. *Journal of Coal*, 04, 3–5.

Ren, H.P. and Fan, J.T. (2016). Adaptive backstepping slide mode control of pneumatic position servo system. *Chinese Journal of Mechanical Engineering*, 29(5), 1003–1009.

Ren, H.P., Fan, J.T., and Kaynak, O. (2019a). Optimal design of a fractional order pid controller for a pneumatic position servo system. *IEEE Transactions on Industrial Electronics*, 66(8), 6220–6228.

Ren, H.P. and Huang, C. (2013a). Adaptive backstepping control of pneumatic servo system. In *Industrial Electronics (ISIE), 2013 IEEE International Symposium on Industrial Electronics*, May, 1–6. IEEE.

Table 1. Tracking error comparison for the sinusoidal signal

Method		Max.RMSE	Avg.RMSE	Max.Q	Avg.Q
Proposed method	positive direction	0.4707	0.4250	1214.2	1112.9
	negative direction	0.4324	0.3855	1267.1	1120.8
Method in Reference [Chiu (2012)]		2.5945	2.3551	1464.2	1419.6
Method in Reference [Ren et al. (2019a)]		1.0858	1.0589	2198.6	2131.8
Method in Reference [Ren et al. (2019b)]		0.7397	0.7108	1284.9	1221.2
Method in Reference [Ren and Fan (2016)]		2.0995	2.0350	2930.4	2930.4
Method in Reference [Nguyen et al. (2007)]		2.5034	2.4804	2930.4	2930.4
Method in Reference [Shtessel et al. (2012)]		2.1966	1.9514	1348.7	1245.2
Method in Reference [Bone and Ning (2007)]		2.5387	2.5144	2862.8	2858.8
Method in Reference [Ren and Huang (2013a)]		2.4579	2.4249	2930.4	2930.4
Method in Reference [Ren and Huang (2013b)]		2.6057	2.5233	2930.4	2930.4
Method in Reference [Bouri and Thomasset (2001)]		2.0675	2.0416	2882.2	2874.7

Table 2. Tracking error comparison for the S-curve signal

Method		Max.RMSE	Avg.RMSE	Max.Q	Avg.Q
Proposed method	positive direction	0.4778	0.4129	1111.2	1106.8
	negative direction	0.4951	0.4120	1102.3	1101.1
Method in Reference [Chiu (2012)]		1.1179	0.9027	1562.9	1503.5
Method in Reference [Ren et al. (2019a)]		0.3291	0.2977	1346.2	1230.5
Method in Reference [Ren et al. (2019b)]		0.3145	0.2640	909.1	874.4
Method in Reference [Ren and Fan (2016)]		0.6263	0.6051	2930.4	2930.4
Method in Reference [Nguyen et al. (2007)]		0.9730	0.9261	2930.4	2930.4
Method in Reference [Shtessel et al. (2012)]		0.7852	0.6461	1518.5	1122.1
Method in Reference [Bone and Ning (2007)]		0.9620	0.9359	2900.6	2904.1
Method in Reference [Ren and Huang (2013a)]		0.8700	0.8147	2930.4	2930.4
Method in Reference [Ren and Huang (2013b)]		0.8955	0.8759	2930.4	2930.4
Method in Reference [Bouri and Thomasset (2001)]		0.6763	0.6502	2783.8	2768.4

Table 3. Tracking error comparison for the multi-frequency sinusoidal signal

Method		Max.RMSE	Avg.RMSE	Max.Q	Avg.Q
Proposed method	positive direction	0.5191	0.4333	1102.5	1100.9
	negative direction	0.4925	0.4258	1105.3	1104.8
Method in Reference [Chiu (2012)]		1.4450	1.2335	1459.1	1404.1
Method in Reference [Ren et al. (2019a)]		0.6781	0.6288	1644.3	1598.5
Method in Reference [Ren et al. (2019b)]		0.6023	0.5739	1031.9	1010.6
Method in Reference [Ren and Fan (2016)]		1.0496	1.0414	2930.4	2930.4
Method in Reference [Nguyen et al. (2007)]		1.3368	1.3059	2930.4	2930.4
Method in Reference [Shtessel et al. (2012)]		1.1925	1.1071	1327.6	1128.9
Method in Reference [Bone and Ning (2007)]		1.3827	1.3316	2921.8	2911.3
Method in Reference [Ren and Huang (2013a)]		1.3250	1.2411	2930.4	2930.4
Method in Reference [Ren and Huang (2013b)]		1.2594	1.2217	2930.4	2930.4
Method in Reference [Bouri and Thomasset (2001)]		1.1059	1.0661	2848.5	2840.7

Ren, H.P. and Huang, C. (2013b). Experimental tracking control for pneumatic system. In *the 2013 IEEE 39th Annual Conference on Industrial Electronics Society*, Vienna, Austria, Nov10–13, 4126–4130. IEEE.

Ren, H.P., Wang, X., Fan, J.T., and Kaynak, O. (2019b). Adaptive backstepping control of a pneumatic system with unknown model parameters and control direction. *IEEE Access*, 7, 64471–64482.

Rubio, J.D.J., Gutierrez, G., Perez, H., and Pacheco, J. (2011). Comparison of three proposed control to accelerate the growth of the crop. *International Journal of Innovative Computing*, 7(7B), 4097–4114.

Sakamoto, M., Matsushita, T., and Mizukami, Y. (2002). Model reference adaptive control using delta-operator with neural network for pneumatic servo system. In *Proceedings of the 2002 SICE 41st Annual Conference*, Osaka, Japan, Aug 5–7, 771–776.

Shtessel, Y., Taleb, M., and Plestan, F. (2012). A novel adaptive-gain supertwisting sliding mode controller: Methodology and application. *Automatica*, 48(5), 759–769.

Yamamoto, A. and Araki (1999). Model reference adaptive control of pneumatic servo system with a constant trace. *Algorithm Journal of Fluid Control*, 2(20), 30–48.

Yong, Y. and Wang, J.H. (2009). A nonlinear feedback tracking control for pneumatic cylinders and experiment study. In *American Control Conference*, Louis, MO, USA, Jun10–12, 3476–3481.

Zhai, L.F., Chai, T.Y., Ge, S., and Lee, T.H. (2008). Stable adaptive neural network control of mimo nonaffine nonlinear discrete-time systems. In *Proceedings of the 47th IEEE Conference, Decision and Control*, Mexico, Dec9–11, 3646–3651.